New Constraints from Haverah Park Data on the Photon and Iron Fluxes of Ultrahigh-Energy Cosmic Rays

M. Ave,[1] J. A. Hinton,[2] R. A. Vázquez,[1] A. A. Watson,[2] and E. Zas[1]
[1]Departamento de Física de Partículas, Universidad de Santiago, 15706 Santiago de Compostela, Spain
[2]Department of Physics and Astronomy, University of Leeds, Leeds LS2 9JT, United Kingdom
(Received 16 March 2000; revised manuscript received 8 August 2000)

Using data from inclined events ($60° < \theta < 80°$) recorded by the Haverah Park shower detector, we show that above 10^{19} eV less than 41% (54%) of the primary cosmic rays can be photons (iron nuclei) at the 95% confidence level. Above 4×10^{19} eV less than 65% of the cosmic rays can be photonic at the same confidence level. These limits place important constraints on some models of the origin of ultrahigh-energy cosmic rays. Details of two new events above 10^{20} eV are reported.

PACS numbers: 98.70.Sa, 96.40.De, 96.40.Pq

The highest energy cosmic rays above the Greisen-Zatsepin-Kuzmin cutoff [1] are a mystery both in terms of their origin and their mass composition. Conventional acceleration mechanisms, so-called "bottom up" scenarios, predict an extragalactic origin with mainly proton composition as, although nuclei of higher charge are more easily accelerated, they are fragile to photonuclear processes in the strong photon fields to be expected in likely source regions [2]. "Top down" (TD) models explain the highest energy cosmic rays as arising from the decay of some sufficiently massive "*X* particles." These models predict particles such as nucleons, photons, and even possibly neutrinos as the high energy cosmic rays, but not heavy nuclei. In some models [3,4] these *X* particles are postulated as long-living metastable superheavy relic particles (MSRP) clustering in our galactic halo. For these MSRP models a photon dominated primary composition at 10^{19} eV is expected. Other top down models [5] associate *X* particles with processes involving systems of cosmic topological defects which are uniformly distributed in the universe, and predict a photon dominated composition only above $\sim 10^{20}$ eV. These models are affected by the constraint that the low energy photons ($\sim$100 MeV) arising from interactions of ultrahigh-energy photons with the cosmic microwave background cannot be larger than the observed diffuse low energy flux [6]. Observations above 10^{19} eV are currently consistent with both interpretations [7,8]. There is however some partial evidence against the photon hypothesis. Shower development of the highest energy event [7] is inconsistent with a photon initiated shower [9] while Akeno Giant Air Shower Array measurements of the muon lateral distribution of the highest energy events are compatible with a proton origin [10]. No measurement of, or limit to, the photon flux above 10^{19} eV has been reported.

Here we describe a new method which we use to set a limit to the photon and iron content of the highest energy cosmic rays. We show that observations of inclined showers provide a powerful tool to discriminate between photon and hadron dominated compositions. For primaries arriving at zenith angles, $\theta > 60°$, the shower particles reaching sea level are almost entirely muons, with a small contamination of electrons and gammas arising mainly from muon decay [11]. From our simulations we find that photons are expected to produce fewer muons than hadrons (a factor of $\sim$9) at 10^{19} eV. This factor decreases with shower energy because of the rise of the photoproduction cross section and the decrease of the pair production and bremsstrahlung cross sections (due to Landau-Pomeranchuk-Migdal suppression [12]). Our conclusions on the photon flux are not sensitive to the choice of model: the implementation of photohadronic interactions in the AIRES code [13] and CORSIKA code [14] (using the parametrization of [15]) gives predictions of the total muon number that are equal to within 10% at 10^{20} eV. In addition, our simulations show that the shape of the lateral distribution of muons in inclined showers is constant with energy and is insensitive to shower to shower fluctuations in longitudinal development [11].

Here we use data from the Haverah Park array, a 12 km^2 array of water-Čerenkov detectors [16]. The data used were recorded between 1974 and 1987 and comprise around 8000 events with $\theta > 60°$ from an on time of 3.6×10^8 s. These events were not analyzed originally because the limited computing power then available required assumptions of circular symmetry which are not valid for inclined showers due to geomagnetic field effects. The analysis described below yielded 46 events with $E > 10^{19}$ eV. Seven events have energies $>4 \times 10^{19}$ eV and two events have energies $>10^{20}$ eV. We show that the rate observed for inclined showers is consistent with a proton dominated primary composition and significantly above that expected if the primary composition is dominated by photons.

Inclined showers recorded at Haverah Park have been analyzed for direction and energy using a combination of Monte Carlo techniques and muon density parametrizations; see [11,17] for details. For zenith angles in the range 60°–89° (in 1° steps) muon density maps were generated using the model [17] with inputs from AIRES for

 0031-9007/00/85(11)/2244(4)$15.00

the QGSJET hadronic model [18] with 10^{19} eV protons. Different azimuth angles are modeled as described in [17]. Throughout we assume the representation of the energy spectrum recently given in [19], noting that the agreement between the fluorescence estimates of the spectrum and those made by other methods implies that we have mass independent knowledge of the spectrum measured in the near-vertical direction. The flux above 10^{19} eV is known to within 20% uncertainty. We find that the lateral and energy distributions of muons in inclined showers are largely independent of primary composition and energy so that simulation of different primary energies and compositions is achieved by scaling the muon density maps described above. We find $N_\mu \propto E^\alpha$ with α equal to 0.924, 0.906, and 1.20 for proton, iron, and gamma primaries, respectively. The relative total muon numbers at 10^{19} eV are 1.0, 1.36, and 0.11 for proton, iron, and gamma primaries, respectively. In general, differences between the lateral distributions and energy spectra of muons in photon and hadronic showers are of particular importance. For inclined showers, however, the differences decrease as the zenith angle increases because the mean height of muon production also increases for both types of primary. At 60°, the lowest zenith angle considered, the differences in the constant density contours are below 20% for distances between 300 and 1000 m. We adopt parameters appropriate to proton primaries to give a conservative estimate of the shower energies by comparison with what would be derived from the assumption of gamma ray primaries. By fitting density maps for proton primaries on an event by event basis we thus obtain equivalent proton energies E_p. For other primaries the energy is related to E_p by an energy dependent multiplicative factor which is $\sim$6 (0.7) for gamma (iron) primaries at $E_p = 10^{19}$ eV, i.e., a photon would require an energy 6 times that of a proton to produce a given density map.

In addition to the electromagnetic contribution due to muon decay, which is present at all core distances at the 20% level for these detectors, the tail of the electromagnetic part of the shower is important at zenith angles below 70° and core distances less than 500 m. This contribution is modeled using AIRES with QGSJET and is radially symmetric in the shower plane. The tail of the electromagnetic part of the shower contributes 10% of the total water-Čerenkov signal at 500 m from the core for a 60° shower.

The Haverah Park arrival directions were determined originally using only the four central triggering detectors [11]. We have reanalyzed the arrival directions of showers having original values of $\theta > 56°$, taking into account all detectors which have timing information. This reanalysis produces smaller arrival direction uncertainties. The rate, as a function of zenith angle, obtained with the new zenith angles, is consistent with predictions [11] showing that the zenith angle reconstruction and the response of the array to inclined showers are well understood.

The curvature of the shower front has been investigated using the AIRES code for inclined showers and found to be consistent with the simple approximation of a spherical front centered on the mean production height of the muons (e.g., at 60° the radius of curvature is 16 km [17]). Beyond $\sim$80° curvature effects are rather small and it is usually sufficient to assume a plane front [20]. When the detected muon number is small there is a systematic effect on the curvature correction and large fluctuations due to limited sampling of the shower front. Therefore, we disregard the timing information from detectors with $<$15 detected equivalent muons. Because of the dependence of the curvature fit on the position of the shower core a three step iteration was needed to give convergence of the core location and direction fits.

The detector signals were measured in units of vertical equivalent muons. Using the GEANT based package, WTANK [21], we find that this unit corresponds to an average number of 14 photoelectrons, consistent with an early experimental estimate of 15 photoelectrons [22]. For inclined showers, additional effects, such as direct light on the photomultiplier tubes, delta rays, and pair production and bremsstrahlung by muons inside the tank, increase this number. For a given zenith angle, the recorded signals are converted into the number of photoelectrons and hence the muon density. The simulations take full account of stopping muons and the resulting decay electrons.

The observed densities were fitted against predictions using the maximum likehood method. Poissonian errors, measurement errors, and errors due to the uncertainty in detector geometry were included. Some events contain saturated detectors which were accounted for using a Gaussian integral for the likelihood function. A three dimensional grid search was made to find the impact point and energy of the shower. The energy was varied in the range $10^{17} < E_p < 10^{21}$ eV in steps of 0.1 in $\log_{10}(E_p/\mathrm{eV})$. The impact point was varied over a grid of 12 km $\times$ 6 km in 40 m steps in the perpendicular plane, the grid asymmetry being necessary to accommodate the ellipticity of inclined showers.

The photoelectron distributions from a water detector show long tails due to the processes mentioned above [11]. We therefore expect an excess of upward over downward fluctuations from the average detector signal. For each event the number of deviations $>2.5\sigma$ expected is calculated from the expected photoelectron distributions. We reject signals having (upward or downward) deviations greater than 2.5σ, recalculating the best fit core after any rejection. Of 211 densities in the events of Table I we rejected 13 upward deviations (the expected number was 17) and rejected 4 densities with downward deviations $>2.5\sigma$.

Errors in the energy and core determination were determined from the likelihood function as in [23]. In addition to this error, an error in energy arises due to the uncertainty in the zenith angle. The error from the zenith angle determination and the error from the fit for core and energy are added in quadrature to give the total errors shown in Table I. To guarantee the quality of events the following cuts were made: (i) the distance from the central triggering

TABLE I. Zenith angle, arrival direction coordinates, and shower energy (assuming proton primary) of selected showers with energy $>4 \times 10^{19}$ eV. MR is the event record number. The reported χ^2 values refer to the energy fits.

MR	Zenith (°)		RA (°)	Dec. (°)	$\log_{10}(E_p/\mathrm{eV})$			χ^2/ν
140 500 50	65	±1.2	86.7	31.7	20.09	−0.15	+0.26	10.3/10
187 316 30	60	±2.3	318.3	3.0	20.06	−0.03	+0.03	45.8/43
141 826 27	70	±1.3	121.2	8.0	19.85	−0.26	+0.42	4.2/10
191 673 20	72	±1.3	152.5	25.9	19.82	−0.06	+0.04	48.4/40
153 010 69	74	±1.2	50.0	49.4	19.78	−0.05	+0.06	26.7/32
127 536 23	74	±2.1	304.9	17.1	19.75	−0.10	+0.06	17.1/11
125 190 70	70	±1.3	47.7	8.8	19.62	−0.08	+0.06	10.2/13

detector to the core position in the shower plane <2 km, (ii) χ^2 probability for the energy and direction fits >1%, and (iii) the downward error in the energy determination be less than a factor of 2. For >80° no showers pass cut (iii).

In Fig. 1 are density maps for two events. These are plotted in the plane perpendicular to the shower direction together with the contours of densities that best fit the data. In each figure the array is rotated in the shower plane such that the y axis is aligned with the component of the magnetic field perpendicular to the shower axis. In the right panel of Fig. 1 the asymmetry in the density pattern due to the geomagnetic field is apparent. For both events the core is surrounded by recorded densities and is well determined. In Table I details are given for seven events with $E_p > 4 \times 10^{19}$ eV.

The data described above are compared to the result expected from different primaries using an input energy spectrum [19] and a Monte Carlo calculation. Figure 2 shows the resulting spectra, for three primary compositions, compared to the data. These simulated spectra are somewhat dependent on the high energy interaction model used. The result is shown for the AIRES air-shower code with the QGSJET interaction model. The SIBYLL hadronic interaction model [24] produces fewer muons than QGSJET (36% less at 10^{19} eV) resulting in reconstructed energies that are higher by ≈40%. Using spectra from the QGSJET model we find that less than 54% of primary cosmic rays above 10^{19} eV can be iron, at a 95% confidence level (assuming a two component mass composition). This bound is however sensitive to the model.

The ratio of photons to protons for MSRP models was first given as typically 10 [3] at 10^{19} eV. However a later model predicts a ratio closer to 2 [4]. On general grounds dominance of photons over protons is expected for these models due to the QCD fragmentation functions of X particles to mesons and baryons. From Fig. 2 we deduce

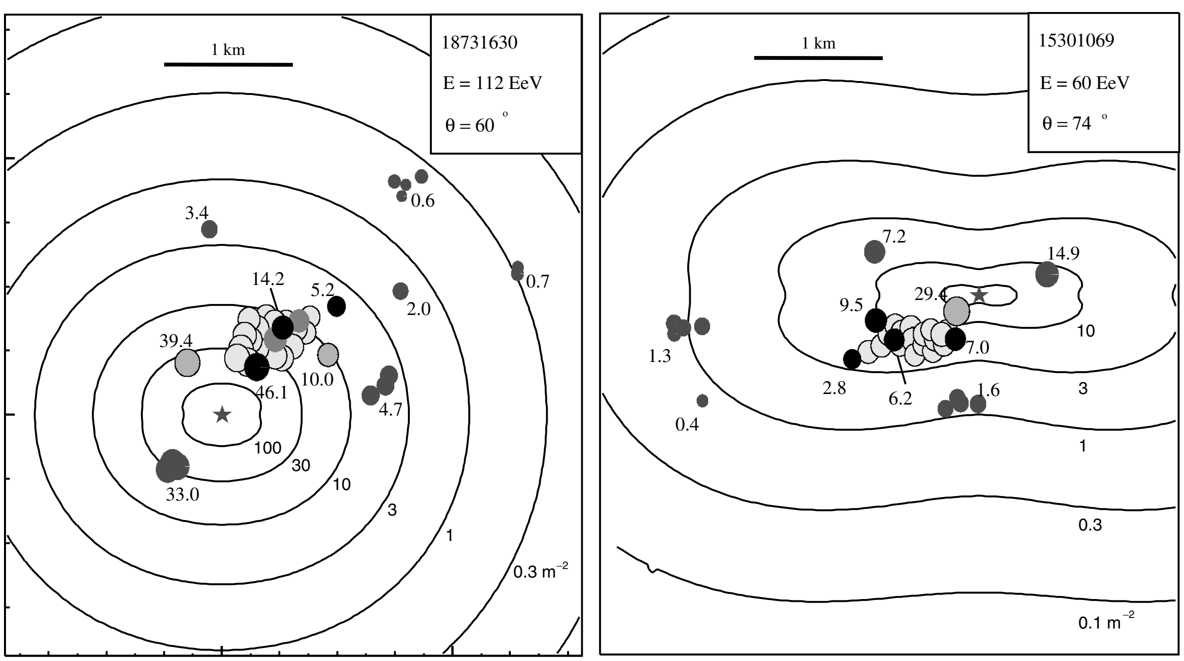

FIG. 1. Density maps of two events in the plane perpendicular to the shower axis. Recorded muon densities are shown as circles with radius proportional to the logarithm of the density. The detector areas are indicated by shading; the area increases from white to black as 1, 2.3, 9, 13, and 34 m^2. The position of the best fit core is indicated by a star. Selected densities are also marked. The y axis is aligned with the component of the magnetic field perpendicular to the shower axis.

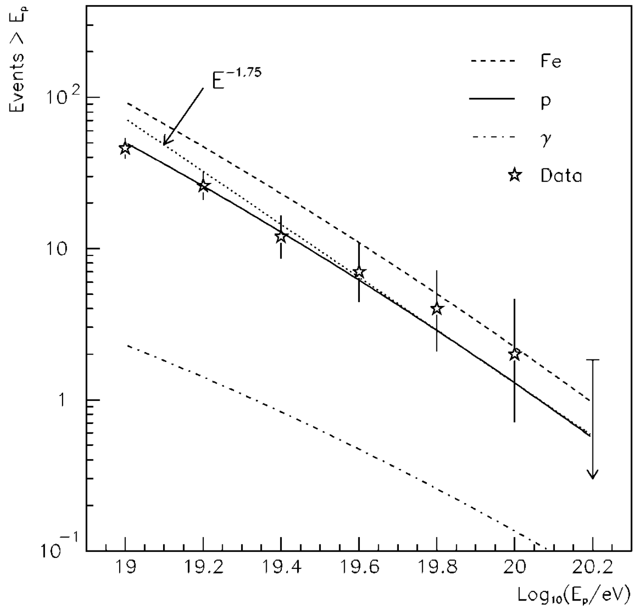

FIG. 2. Integral number of inclined events as a function of energy for the Haverah Park data set compared to the predictions for iron, protons, and photon primaries. Here the energy is calculated assuming a proton primary. The slope of the assumed primary spectrum ($E^{-1.75}$) is shown to illustrate the increase of trigger efficiency with energy.

that above 10^{19} eV less than 41% of the primary cosmic rays can be photons, with a 95% confidence level. Above 4×10^{19} eV less than 65% can be photons at the same confidence level. Here we have assumed that downward or upward fluctuations from the observed integral numbers by 2 standard deviations could be accounted for by appropriate contributions of protons plus gamma rays or protons plus iron nuclei, respectively.

These limits set important constraints to TD mechanisms as the origin of the highest energy cosmic rays. We note also that the gamma/proton ratio predicted to arise from proton interactions with the 2.7 K background radiation is 30% at 10^{19} eV when it is assumed that the protons are produced universally with a differential slope of 2 and a maximum energy of 10^{21} eV [25]. With the Southern Auger Observatory (3000 km^2) a ratio as small as 10% could be explored at 10^{19} eV with 3 years of data using this new technique.

Our photon bound is also conservative because we have not taken into account the interactions of the high energy photons in the magnetic field of the earth [26]. This has the effect of converting a single energetic photon into a few lower energy photons. As the total number of muons in a shower initiated by a single photon scales with $E^{1.2}$, the number of muons in a shower initiated by a single photon exceeds the total number of muons in the multiple photon showers of lower energy.

This work was partly supported by a joint grant from the British Council and the Spanish Ministry of Education (HB1997-0175), by Xunta de Galicia (XUGA-20604A98), by CICYT (AEN99-0589-C02-02), and by PPARC(GR/L40892). We thank J. W. Cronin, F. Halzen, J. Lloyd-Evans, and A. W. Wolfendale for critical readings of the manuscript. We also thank the authors of the AIRES and CORSIKA codes.

[1] K. Greisen, Phys. Rev. Lett. **16**, 748 (1966); Z. T. Zatsepin and V. A. Kuzmin, Pis'ma Zh. Eksp. Teor. Fiz. **4**, 144 (1966) [Sov. Phys. JETP Lett. **4**, 78 (1966)].
[2] A. M. Hillas, Annu. Rev. Astron. Astrophys. **22**, 425 (1984).
[3] V. S. Berezinsky, M. Kachelriess, and A. Vilenkin, Phys. Rev. Lett. **79**, 4302 (1997).
[4] M. Birkel and S. Sarkar, Astropart. Phys. **9**, 297 (1998).
[5] P. Bhattacharjee, C. T. Hill, and D. N. Schramm, Phys. Rev. Lett. **69**, 567 (1992).
[6] X. Chi, C. Dahanayake, J. Wdowczyk, and A. W. Wolfendale, Astropart. Phys. **1**, 129 (1992); R. J. Protheroe and T. Stanev, Phys. Rev. Lett. **77**, 3708 (1996).
[7] D. Bird *et al.,* Astrophys. J. **441**, 144 (1995).
[8] N. Hayashida *et al.,* Phys. Rev. Lett. **73**, 3491 (1994).
[9] F. Halzen, R. A. Vazquez, T. Stanev, and H. P. Vankov, Astropart. Phys. **3**, 151 (1995).
[10] M. Nagano, D. Heck, K. Shinozaki, N. Inoue, and J. Knapp, astro-ph/9912222 [Astropart. Phys. (to be published)].
[11] M. Ave, J. A. Hinton, R. A. Vazquez, A. A. Watson, and E. Zas, astro-ph/0003011 [Astropart. Phys. (to be published)].
[12] L. Landau and I. Pomeranchuk, Dokl. Akad. Nauk SSSR **92**, 535 (1953); **92**, 735 (1953); A. B. Migdal, Phys. Rev. **103**, 1811 (1956); Sov. Phys. JETP **5**, 527 (1957).
[13] S. J. Sciutto, in *Proceedings of the XXVI International Cosmic Ray Conference, Salt Lake City, 1999* (AIP, New York, 2000), Vol. 1, p. 411.
[14] D. Heck, J. Knapp, J. N. Capdevielle, G. Shatz, and T. Thouw, Forschungzentrum Karlsruhe Report No. FZKA 6019, 1998.
[15] T. Stanev, T. K. Gaisser, and F. Halzen, Phys. Rev. D **32**, 1244 (1985).
[16] M. A. Lawrence, R. J. O. Reid, and A. A. Watson, J. Phys. G **17**, 733 (1991).
[17] M. Ave, R. A. Vazquez, and E. Zas, Astropart. Phys. (to be published).
[18] N. N. Kalmykov and S. S. Ostapchenko, Yad. Fiz. **56**, 105 (1993); Phys. At. Nucl. **56**, 346 (1993).
[19] M. Nagano and A. A. Watson, Rev. Mod. Phys. (to be published).
[20] X. Bertou, P. Billior, and T. Pradier, GAP Note 58 (1997), see http://www.auger.org/admin/.
[21] J. R. T. de Mello Neto, GAP Note 20 (1998), see http://www.auger.org/admin/.
[22] A. J. Baxter, Ph.D. thesis, University of Leeds, 1967, p. 24.
[23] M. Lampton, B. Margon, and S. Bowyer, Astrophys. J. **208**, 177 (1976).
[24] R. T. Fletcher, T. K. Gaisser, P. Lipari, and T. Stanev, Phys. Rev. D **50**, 5710 (1994); J. Engel, T. K. Gaisser, P. Lipari, and T. Stanev, Phys. Rev. D **46**, 5013 (1992).
[25] J. Wdowczyk and A. W. Wolfendale, Astrophys. J. **349**, 35 (1990).
[26] B. McBreen and C. J. Lambert, Phys. Rev. D **24**, 2536 (1981); X. Bertou, P. Billior, and S. Dagoret-Campagne, Astropart. Phys. (to be published).